Photosynth Res (2017) 133:317–326
DOI 10.1007/s11120-017-0352-4

ORIGINAL ARTICLE

Energy transfer in *Anabaena variabilis* filaments adapted to nitrogen-depleted and nitrogen-enriched conditions studied by time-resolved fluorescence

Aya Onishi[1] · Shimpei Aikawa[2] · Akihiko Kondo[2] · Seiji Akimoto[1,3]

Received: 24 October 2016 / Accepted: 7 February 2017 / Published online: 16 February 2017

Abstract Nitrogen is among the most important nutritious elements for photosynthetic organisms such as plants, algae, and cyanobacteria. Therefore, nitrogen depletion severely compromises the growth, development, and photosynthesis of these organisms. To preserve their integrity under nitrogen-depleted conditions, filamentous nitrogen-fixing cyanobacteria reduce atmospheric nitrogen to ammonia, and self-adapt by regulating their light-harvesting and excitation energy-transfer processes. To investigate the changes in the primary processes of photosynthesis, we measured the steady-state absorption and fluorescence spectra and time-resolved fluorescence spectra (TRFS) of whole filaments of the nitrogen-fixing cyanobacterium *Anabaena variabilis* at 77 K. The filaments were grown in standard and nitrogen-free media for 6 months. The TRFS were measured with a picosecond time-correlated single photon counting system. Despite the phycobilisome degradation, the energy-transfer paths within phycobilisome and from phycobilisome to both photosystems were maintained. However, the energy transfer from photosystem II to photosystem I was suppressed and a specific red chlorophyll band appeared under the nitrogen-depleted condition.

✉ Seiji Akimoto
akimoto@hawk.kobe-u.ac.jp

[1] Graduate School of Science, Kobe University, Kobe 657-8501, Japan

[2] Graduate School of Engineering, Kobe University, Kobe 657-8501, Japan

[3] Molecular Photoscience Research Center, Kobe University, Kobe 657-8501, Japan

Keywords Energy transfer · Time-resolved fluorescence · Nitrogen depletion · Nitrogen-fixing cyanobacteria · Red chlorophyll

Abbreviations

APC	Allophycocyanin
Car	Carotenoid
Chl	Chlorophyll
FDAS	Fluorescence decay-associated spectra
PC	Phycocyanin
PS	Photosystem
PBS	Phycobilisome
TRFS	Time-resolved fluorescence spectra

Introduction

Cyanobacteria constitute a large group of photosynthetic prokaryotes. Like their photosynthetic eukaryotic counterparts (algae and plants), their thylakoid membrane contains two transmembrane pigment–protein complexes called photosystem I (PSI) and photosystem II (PSII), which enable light-driven oxygenic photosynthesis (Blankenship 2014). Besides possessing both photosystems (PSs), cyanobacteria retain a light-harvesting antenna pigment–protein complex called phycobilisome (PBS) on their thylakoid membrane surface (Gantt and Conti 1969), which comprises a rod and a core. The excitation energy captured by PBS is efficiently transferred to PSI or PSII, and transfers from the rod to the core of the PBS under an energy gradient (Allen and Holmes 1986). These pigment–protein complexes contain a remarkable number of photosynthetic pigments, which are broadly classified into three types: chlorophyll *a* (Chl *a*), carotenoids (Cars), and bilins. Chl *a* and some Cars are located in PSI and PSII and some bilins are associated with

PBS (Blankenship 2014). In the primary process of photosynthesis, the excitation energy captured by these pigments is transferred to their reaction center (P700 in PSI and P680 in PSII).

Owing to their high adaptability, cyanobacteria are widely distributed and can survive in dramatically fluctuating local environments (Blankenship 2014). Unfortunately, most cyanobacteria grow under sub-optimal conditions in nature and are often subjected to environmental stressors such as light intensity and/or quality, low nutrient availability, and adverse temperature or pH (Gantt 1975; Fogg 2001). To avoid serious damage and to ensure survival under unfavorable conditions, cyanobacteria adapt by regulating their primary photosynthetic process (Gantt 1975). Thus, cyanobacteria are regarded as model organisms for studying adaptive responses to various environmental stresses, and have been widely used in photosynthetic research.

As cyanobacteria derive their energy from light and inorganic nutrients, inorganic nutrient deprivation is the limiting factor in their growth, development, and photosynthesis (Grossman et al. 1994). Inorganic nutrients are roughly divided into macronutrients and micronutrients. Deficiency of macronutrients such as nitrogen, sulfur, and phosphorus induces PBS degradation (Collier and Grossman 1992, Schwarz and Forchhamme 2005), and affects the excitation energy-transfer processes within and between the pigment–protein complexes. The effects of macronutrient deprivation have been investigated in the cyanobacterium *Synechococcus* sp. PCC 7942 grown in nitrogen-, sulfur- or phosphorus-free medium (replacing the $NaNO_3$, $MgSO_4$, or K_2PO_4 salts with NaCl, $MgCl_2$, or KCl, respectively). Collier et al. (1994) suggested that under nutrient-poor conditions, the light energy absorbed by the PBS is not efficiently transferred to Chl, but is largely fluoresced from the PBS terminal emitter. Micronutrients also affect the photosynthetic processes. Niki et al. reported that energy-transfer processes were affected by nutrients other than NO_3^- under both nitrogen-rich and nitrogen-deficient conditions (Niki et al. 2015). Under iron-deficient conditions, additional antenna complexes containing Chl *a*, which work as light-harvesting antennae of PSI, form around the PSI trimers (Laudenbach and Straus 1988; Michel and Pistorius 2004). Calcium-deficient conditions suppress the excitation energy transfer in the PBS rods and cause quenching at the ends of the rods (Yokono et al. 2012a).

As a main constituent of amino acids, photosynthetic pigments, and nucleic acids, nitrogen is especially important for photosynthesis, and occupies approximately 10% of the dry weight of a cyanobacterial cell (Cobb and Myers 1964). Representative nitrogen sources are ammonium, nitrate, and nitrite. In the absence of nitrogen, non-diazotrophic cyanobacteria source nitrogen by degrading their own PBS (Grossman et al. 1993). During long-term nitrogen depletion, the altered pigment composition manifests as a color change of the culture medium from blue–green to yellow. Additionally, nitrogen stress influences the absorption intensity and excitation energy transfer from phycocyanin (PC) to Chl *a* in intact *Arthrospira* (*Spirulina*) *platensis* filaments grown in low-nitrate medium ($NaNO_3$ levels below 1/500 that of standard medium) (Peter et al. 2010).

Diazotrophic (nitrogen-fixing) cyanobacteria avoid the adverse effects of nitrogen depletion by reducing atmospheric nitrogen to ammonia (Fay 1992; Postgate 1998). However, the nitrogen-fixation enzyme (nitrogenase) is irreversibly inactivated by molecular oxygen (Wolk 1996; Postgate 1998). Thus, diazotrophic cyanobacteria have evolved strategies to protect their nitrogenase from molecular oxygen. In filamentous diazotrophic cyanobacteria such as *Anabaena* and *Nostoc*, the photosynthesis and nitrogen-fixation processes are spatially separated by heterocysts derived from vegetative cells (Berman-Frank et al. 2003; Kumar et al. 2010). Heterocysts are specialized cells for nitrogen fixation, and are characterized by a thick membrane, high PSI activity, and loss of division capability (Maldener and Muro-Pastor 2010).

Previous studies have investigated photosynthesis in isolated heterocysts of *Anabaena* and *Nostoc*, and have documented the degradation of PBS and PSII under nitrogen stress and during heterocyst differentiation. Although pigments are usually quantified by physiological and biochemical methods, the isolation procedures may influence the pigment–pigment, pigment–protein, and/or complex–complex interactions. Each PSI monomer contains 9–11 red Chls, which absorb longer-wavelength light than P700 (Boardman et al. 1966; Goedheer 1972; Nakayama et al. 1979; Govindjee 2004) by excitonic coupling of the Chl *a* molecules. Red Chls reportedly play important roles in the primary process of photosynthesis (Pålsson et al.1998; Jordan et al. 2001). Therefore, isolation will likely affect some of the energy transfers among the Chls. Furthermore, the pigment quantities and interactions depend on the growth and differentiation stages, which differ among the cells (Thomas 1970; Ying et al. 2002). Some isolation methods may select heterocysts beyond a certain stage of maturity (Ferimazova et al. 2013). For these reasons, in vivo measurements are important for studying the primary process of photosynthesis.

In our previous study, we reported modified pigment compositions and the energy-transfer processes in nitrogen-deprived intact filaments of *Anabaena variabilis* throughout their growth period in 15 days after the nitrogen depletion without another inoculation. The investigation was performed by a spectroscopic method (Onishi et al. 2015). The growing filaments gradually changed their photosynthetic process. In the present study, we investigate the

in vivo energy-transfer processes of *A. variabilis* filaments adapted to nitrogen-depleted or nitrogen-enriched conditions for 6 months with repeated inoculations. To this end, we measure and analyze the steady-state absorption and fluorescence spectra and time-resolved fluorescence spectra (TRFS). Time-resolved fluorescence spectroscopy detects only the signals from excited-state pigments, revealing the excitation energy-transfer processes at different times after excitation. By comparing the filaments grown under nitrogen-depleted and nitrogen-enriched conditions, we can understand the nitrogen stress response of the filamentous diazotrophic cyanobacterium *A. variabilis*.

Materials and methods

Culture conditions

The filamentous cyanobacterium *A. variabilis* ATCC 29,413 was continuously cultivated in modified BG11 medium or BG11 medium without $NaNO_3$ ($BG11_0$ medium) for 6 months to acclimate to each nitrate condition. Part of cultured cells were transferred to fresh media once every 1–2 weeks (at 0.04 of the optical density at 750 nm). Each liter of BG11 medium contained 1.5 g $NaNO_3$, 0.04 g K_2HPO_4, 0.075 g $MgSO_4$ H_2O, 0.036 g $CaCl_2$ $2H_2O$, 0.006 g citric acid, 0.006 g ferric citrate, 0.001 g EDTA (disodium salt), 0.02 g Na_2CO_3, 2.86 mg H_3BO_3, 1.81 mg $MnCl_2$ $4H_2O$, 0.222 mg $ZnSO_4$ $7H_2O$, 0.39 mg $NaMoO_4$ $2H_2O$, 0.079 mg $CuSO_4$ $5H_2O$, and 49.4 µg $Co(NO_3)_2$ $6H_2O$. *Anabaena variabilis* cells were cultivated in 200 mL Erlenmeyer flasks containing 70 mL of BG11 or $BG11_0$ with 100 rpm agitation under continuous illumination at 40 µmol photons m^{-2} s^{-1} using white fluorescent bulbs (Life look HGX and NHG; NEC Corporation, Tokyo, Japan), with air conditioning to maintain a temperature of 30 °C in a bio-shaker (BR-40LF, TAITEC, Tokyo, Japan). The *A. variabilis* cells were measured 4 days after inoculating to fresh media. The cultured cells in BG11 and $BG11_0$ were referred to as N+ and N−, respectively.

Measurement of steady-state spectra

Steady-state absorption spectra were measured by a spectrometer equipped with an integrating sphere (V-650/ISVC-747, JASCO, Tokyo, Japan) at 77 K, and steady-state fluorescence spectra were measured with a spectrofluorometer (FP-6600/PMU-183, JASCO, Tokyo, Japan) at 77 K. The excitation wavelengths were 440 and 600 nm, which mainly excite the Chl Soret band and PC, respectively. Samples for steady-state fluorescence measurements were prepared under dimly light conditions, and homogenous ice was obtained by adding polyethylene glycol (average molecular weight 3350, final concentration 15% (w/v), Sigma-Aldrich, USA) to the sample solutions.

Measurement of time-resolved fluorescence spectra

Time-resolved fluorescence spectra (TRFS) were measured by a time-correlated single photon counting system operated at 77 K (Akimoto et al. 2012). The excitation source was a picosecond diode laser (PiL040X, Advanced Laser Diode Systems, Germany). The excitation wavelength (408 nm) simultaneously excites all pigments. The time interval for data acquisition was set to 2.44 ps/channel (total time window = 10 ns) or 24.4 ps/channel (100 ns) and the repetition rate of the pulse picker was 5.0 MHz. Therefore, the measurements were unaffected by excitation pulses up to 100 ns. The width of the instrumental response function was approximately 50 ps. The fluorescence kinetics were measured from 620 to 770 nm at 1-nm intervals. Fluorescence behaviors were consistent in repeated measurements, confirming constant sample conditions throughout the measurements. Samples were prepared as described for the steady-state fluorescence measurements. In the TRFS measurements, the fluorescence from the sample surface was monitored at right angles to the incident light.

Results

Steady-state absorption and fluorescence spectra

Figure 1 shows the steady-state absorption spectra of *A. variabilis* filaments at 77 K. All absorption spectra were normalized at 678 nm. The Chl absorption peaks at 440, 678, and 710 nm, correspond to the Chl Soret band, the Chl Qy(0, 0) band, and the lower-energy Chl (red-Chl) band

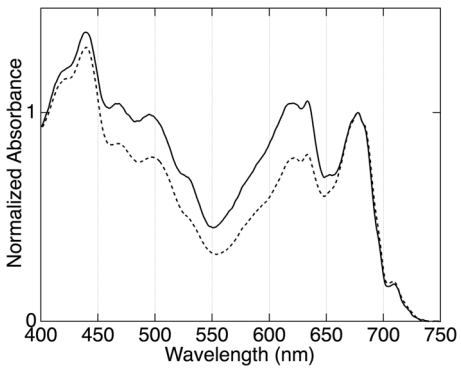

Fig. 1 Steady-state absorption spectra of *Anabaena variabilis* filaments grown under nitrogen-enriched conditions (N+, *solid line*) and nitrogen-depleted conditions (N–, *dotted line*) at 77 K. The spectra were normalized at the Chl Qy(0, 0) band

Table 1 Intensity ratios in the steady-state absorption spectra (Fig. 1) of *Anabaena variabilis* filaments grown under nitrogen-enriched conditions (N+) and nitrogen-depleted conditions (N–) at 77 K

Samples	Car_{495}/Chl_{678}	PC_{620}/Chl_{678}*	Chl_{708}/Chl_{678}
N+	0.99	0.84	0.18
N−	0.79	0.58	0.19

Car_{495}, PC_{620}, Chl_{678}, and Chl_{708} denote carotenoid (495 nm), phycocyanin (620 nm), chlorophyll (678 nm), and lower-energy chlorophyll (708 nm), respectively

*The values of PC_{620}/Chl_{678} were obtained by subtracting the estimated contribution of the Chl Qy(1, 0) band (0.20) from the apparent relative absorbance around 620 nm

of PSI, respectively. The three peaks around 500 nm are assigned to Car. The peaks at 620 and 632 nm are attributed to PC, and the shoulder around 655 nm is assigned to allophycocyanin (APC). The relative intensities of the Car, PBS, and PSI red-Chl bands (Car_{495}/Chl_{678}, PBS_{620}/Chl_{678}, and Chl_{708}/Chl_{678}, respectively) depend on the cultivation media (see Table 1). The Qy(1, 0) absorption band of Ch1 appears around 620 nm. To estimate the PBS_{620}/Chl_{678}, we assumed identical intensity ratio of the Qy(1, 0) band to the Qy(0, 0) band in all intact cells, and that PSI and PSII are isolated. Therefore, we used the relative intensity of the Chl Qy(1, 0) band and subtracted 0.20 from the apparent relative absorbance around 620 nm. In the nitrogen-depleted medium, adaptation by the *A. variabilis* filaments was revealed by four notable changes in the absorption spectrum: decreased relative intensity of the Car band, a 3–4 nm redshift of the Car band, decreased relative intensity of the PBS band, and slightly increased relative intensity of the PSI red-Chl band. The major Cars of *A. variabilis* are *β*-carotene (51%), echinenone (20%), and canthaxanthin (22%) (Takaichi et al. 2006). During long-term growth in nitrogen-free medium, the proportion of lower-energy Cars increased, suggesting an adaptive response to nitrogen deprivation by the *A. variabilis* filaments.

Figure 2 shows the steady-state fluorescence spectra of *A. variabilis* filaments at 77 K. The excitation wavelength was 440 nm (Fig. 2a, Chl excitation) and all fluorescence spectra were normalized at the PSI red-Chl band (~730 nm; Govindjee and Yang 1966). Excitation at 440 nm induces a large peak around 730 nm in the PSI fluorescence region, with additional bands in the 680–700 nm region. The peaks around 685 and 695 nm are attributed to the core antenna complexes CP43 and CP47 of the PSII reaction center, respectively (Murata and Satoh 1986). The relative fluorescence intensity of PSI to PSII is lower in the nitrogen-deprived filaments than in those grown in standard medium. Under 600-nm excitation, additional peaks appear around 650 and 665 nm, which are attributed to PC and APC, respectively (Fig. 2b, PC excitation). In the PBS

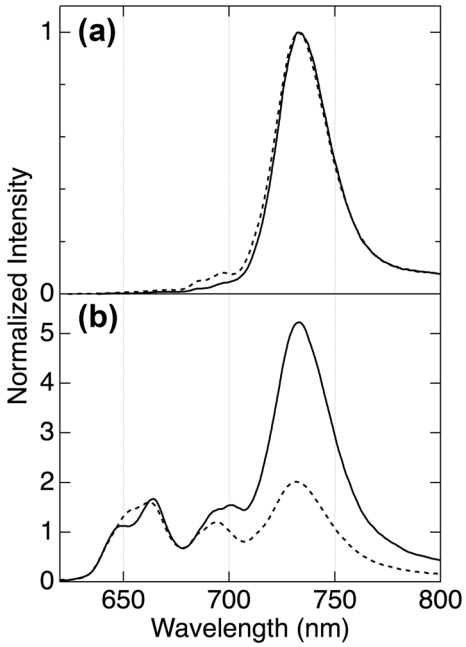

Fig. 2 Steady-state fluorescence spectra of *Anabaena variabilis* filaments grown under nitrogen-enriched conditions (N+, *solid line*) and nitrogen-depleted conditions (N–, *dotted line*) at 77 K. Excitation wavelength was 440 nm (**a**) or 600 nm (**b**). The spectra were normalized at the PSI red-Chl band (**a**) or by the shorter wavelength side of the PC band (**b**)

fluorescence region, the N− spectrum shows decreased relative fluorescence intensity of PSI to PBS and a longer-wavelength shift of the PC peak. Both samples emit from PSI and PSII in the Chl fluorescence region, indicating that the excitation energy captured by PBS is efficiently transferred to both PSII and PSI, regardless of nitrogen availability. However, the relative fluorescence intensity of PSI to PSII is smaller in N− than in N+ (Table 2), indicating that the energy distributions are differently proportioned in N+ and N−; that is, PBS transfers less excitation energy to PSI under long-term nitrogen depletion.

Time-resolved fluorescence spectra and fluorescence decay-associated spectra

Figure 3 shows the TRFS of *A. variabilis* filaments at 77 K. All fluorescence spectra were normalized at ~730 nm (the PSI red-Chl band). Under 408 nm (which excites all pigments), another four fluorescence peaks appear around 650, 665, 685, and 695 nm. The former two are assigned to PC and APC, respectively; the latter two are assigned to red Chl in CP43 and CP47 of PSII, respectively. The relative fluorescence intensity of PBS is lower in N− than in N+ during the early time range (0–5 ps), but is higher in N− in the 3.1–3.5 ns range, despite the reduced relative amount of PBS (Fig. 1). Conversely, in the Chl

Table 2 Fluorescence intensity ratios (PSI/PSIIs) in the steady-state fluorescence (SF) spectra excited at 600 nm (Fig. 2b), and the delayed fluorescence (DF) spectra (Fig. 4)

Samples	PSI/PSII in SF	PSI/PSII in DF	ΔPSI/PSII
N+	4.8	3.8	1.0
N−	2.7	1.8	0.9

In both spectra, PSII and PSI peak around 695 and 733 nm, respectively. Considering the differences in fluorescence quantum yields, we divided the apparent PSI/PSII ratios by the corresponding mean lifetimes

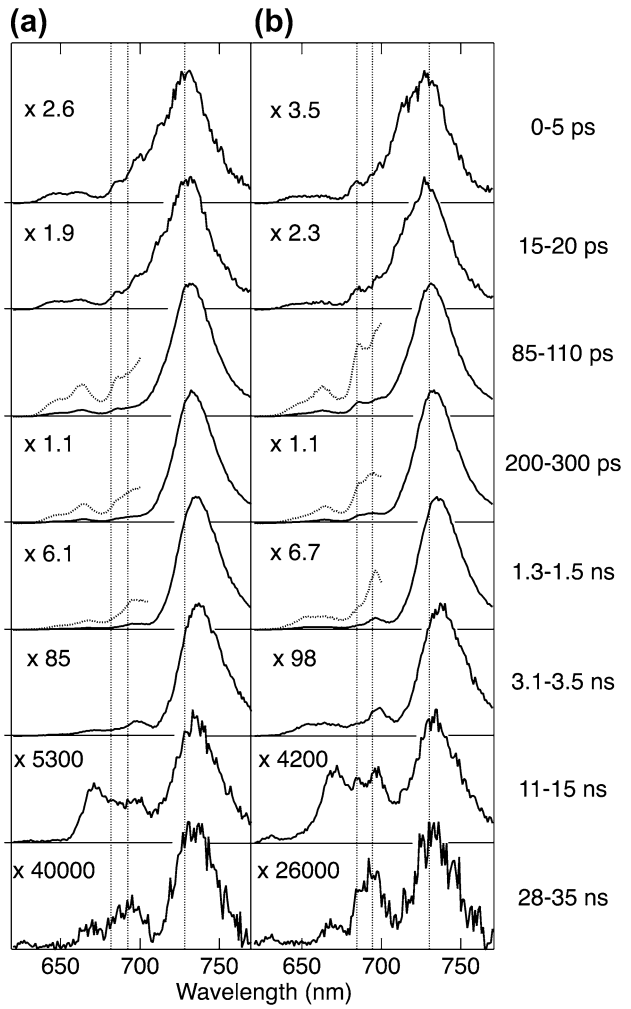

Fig. 3 Time-resolved fluorescence spectra of *Anabaena variabilis* filaments grown under nitrogen-enriched conditions (N+) (**a**) and nitrogen-depleted conditions (N–) (**b**) at 77 K. The excitation wavelength was 408 nm, and each spectrum was normalized by its maximum intensity. *Dotted lines* are ×5 magnifications of the original spectra. *Numbers* shown on individual spectra indicate the magnification factors relative to the most intense spectrum. The *gray vertical lines* indicate 685, 695, and 730 nm from *left to right*

fluorescence region of N−, the PSI red-Chl peak shifts to a shorter wavelength (726 nm) immediately after laser excitation (0–5 ps in Fig. 3), and the relative fluorescence intensities around 710 nm are higher in N− than in N+. Over time, the peak positions in the PSI red-Chl fluorescence region shift to longer wavelengths, and the fluorescence maxima of N+ and N− coincide after 85 ps. In the final TRFS (28–35 ns in Fig. 3), both samples display PSII and PSI peaks, but the PSI/PSII ratio in N− is almost half that of N+.

Figure 4 shows the fluorescence decay-associated spectra (FDAS). The fluorescence curves were fitted by sums of exponentials with seven common time constants: 10–20 ps, 65–85 ps, 220–280 ps, 480–590 ps, 1.1–1.7 ns, 4.8–5.1 ns, and over 16–20 ns. The fitting formula is given by

$$F(t,\lambda) = \sum_{n=1}^{7} A_n(\lambda) \exp\left(-\frac{t}{\tau_n}\right).$$

Before constructing FDAS, fluorescence decay curves were deconvoluted using free-running exponential components with an instrument function. The positive and negative amplitudes A_n (λ) in the spectra correspond to the fluorescence decay and rise components, respectively. Therefore, a positive and negative pair of peak amplitudes indicates that energy is transferred from a pigment with positive amplitudes to one with negative amplitudes (Akimoto et al. 2012). In the PBS fluorescence region of the first FDAS (the 10–20 ps components; see Fig. 4), N+ and N− exhibit a positive–negative amplitude pair around 645 nm (PC) and 665 nm (APC), respectively, indicating that energy transfers from PC to APC even under nitrogen-depleted conditions. The amplitudes of the peak around 685 nm (PSII red Chl) of the first FDAS are positive in N+ but negative in N−. In the PSI red-Chl region of the first FDAS, both samples exhibit a pair of positive and negative amplitudes, but their spectra differ in two notable ways. First, whereas N− exhibits two positive peaks (~695 and ~710 nm), the longer-wavelength peak (~710 nm) is absent in N+. Second, the negative peak appears at longer wavelength in N− (~735 nm) than in N+ (~725 nm). In the second FDAS (the 65–85 ps components, Fig. 4), both samples exhibit a fluorescence peak with negative amplitude in the PSI red-Chl region (~735 nm). In the third FDAS (the 220–280 ps components, Fig. 4), N+ exhibits a positive–negative pair of amplitudes, whereas all N− amplitudes are positive. The fluorescence maxima in the fourth and fifth FDAS (the 480–590 ps and 1.1–1.7 ns components, respectively, in Fig. 4) almost coincide, indicating very similar energies of the red PSI Chls in both samples (~735 nm and ~739 nm in the fourth and fifth FDAS, respectively). The seventh FDAS (the 16–20 ns components in Fig. 4), called the delayed fluorescence spectrum,

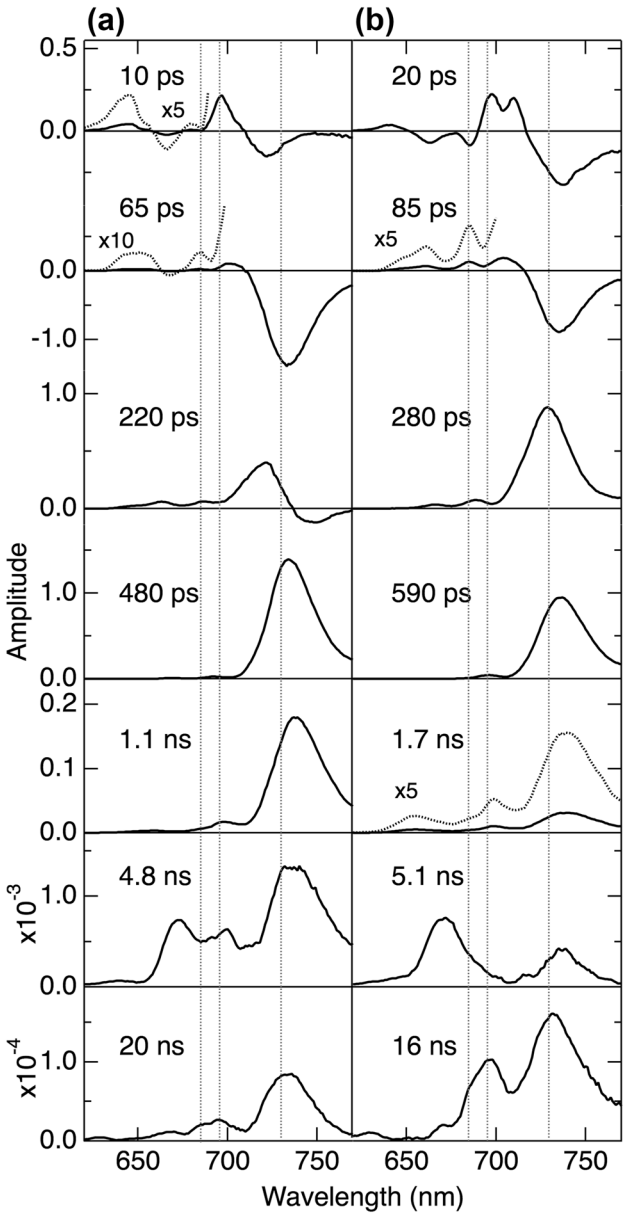

Fig. 4 Fluorescence decay-associated spectra of *Anabaena variabilis* filaments grown under nitrogen-enriched conditions (N+) (**a**) and nitrogen-depleted conditions (N–) (**b**), obtained by global analysis of the time-resolved fluorescence spectra (Fig. 3). *Dotted lines* are magnified by the factors displayed in each window. The *gray vertical lines* indicate 685, 695, and 730 nm from *left to right*

reveals the long-lived fluorescences with time constants exceeding the lifetime of an isolated Chl molecule (~6 ns). Delayed fluorescence originates from re-generation of an excited state by charge recombination in the PSII reaction center (Mimuro et al. 2007). The charge separation in the PSI reaction center, caused by rapid electron transfer from the primary to the secondary electron acceptor, is essentially irreversible (Mimuro et al. 2010). Therefore, delayed fluorescence in the PSI fluorescence region is detectable only during direct PSII→PSI energy transfer. In the present study, the relative PSI/PSII ratios in the delayed fluorescence spectra of N+ and N− were 4.8 and 2.7, respectively (Table 2).

Discussion

Excitation energy-transfer process in PBS

In the steady-state absorption spectra (Fig. 1), the PBS content (relative to the Chl Qy band) was ~30% lower in N− than in N+ (see Table 1). This indicates that the PBS of *A. variabilis* was degraded under nitrogen-depleted conditions. Similar degradation was reported in the non-diazotrophic cyanobacterium *Anacystis nidulans* (Allen and Smith 1969), *Synechococcus* sp. PCC 7942 (Collier et al. 1994; Görl et al. 1998), and *A. platensis* (Peter et al. 2010). Although both diazotrophic and non-diazotrophic cyanobacteria degrade their light-harvesting antenna when starved of nitrogen, the degree of PBS degradation and the excitation energy-transfer processes in the PBS differ between the two types. In non-diazotrophic cyanobacteria, the PBS is degraded to non-detectable levels under long-term nitrogen deprivation. Nitrogen-deprived cells of *Synechococcus* sp. PCC 7942 reduce their PBS/Chl ratio to ~10% that of cells grown in standard medium (Collier and Grossman 1992). In contrast, nitrogen-deprived diazotrophic cyanobacteria such as *Anabaena* and *Nostoc* retain most of their PBS, and sometimes recover their nominal PBS levels after degradation under certain growth conditions (Thomas 1972, Ehira and Ohmori 2006).

PBS degradation affects the excitation energy-transfer processes within the PBS. After PBS degradation, the relative fluorescence intensity from the PC region increases in the steady-state fluorescence spectra (Fig. 2b) and in the later time region of the TRFS (3.1–3.5 ns, Fig. 3). Overall, these results suggest that much of the excitation energy is emitted as fluorescence from the PBS rod, reducing the efficiency of PC→APC energy transfer. However, in the first FDAS (the 10–20 ps components of Fig. 4), a positive (~645 nm) and negative (~665 nm) amplitude pair appears in both samples. This positive–negative pair of amplitudes indicates that under nitrogen-depleted conditions, the PC→APC energy transfer is maintained by nitrogen fixation. Therefore, nitrogen depletion appears to affect the slower energy-transfer path, leaving the rapid energy-transfer path intact. PBS peak(s) are absent in the 7th FDAS (the 16–20 ns components of Fig. 4), indicating that negligibly small excitation energy remains in the PBS. This situation contrasts with the energy transfer under salinity stress (Arba et al. 2013).

Excitation energy transfer within photosystems

Among the ~100 Chl *a* molecules contained in the PSI monomer, 9 – 11 undergo strong interactions, and hence absorb light at longer wavelengths than P700. Each of these Chls, called red Chls, possesses a slightly different energy (Jordan et al. 2001). According to numerous studies on widely varying cyanobacterial species, the numbers and energies of red Chls are species-specific (Pålsson et al. 1998). At room temperature, the uphill excitation energy transfer from red Chls to P700 is efficient and absorption cross section of PSI in the longer-wavelength region increases (Trissl et al. 1993). At 77 K, excitation energy is also transferred from higher-energy to lower-energy red Chls in PSI, and the fluorescence emission is dominated by red Chls. Additionally, many β-carotene molecules are localized near red Chls (Jordan et al. 2001), which perform light harvesting and quenching against excess excitation (Mimuro and Katoh 1991).

The spectral shape of FDAS (Fig. 4) reveals at least four spectral components in the PSI region: antenna band (~695 nm) and three types of red-Chl bands, R1 band (700 – 710 nm), R2 band (720 – 730 nm), and R3 band (735 – 740 nm). The first FDAS (the 10–20 ps components, Fig. 4) exhibits antenna bands in both samples, but the R1 band exists only in N–. This result is consistent with our previous study, in which the R1 band was consistently observed in nitrogen-depleted medium, but was never detected in nitrogen-enriched medium (Onishi et al. 2015). This suggests that the R1 band is a spectral indicator of filaments grown under nitrogen-depleted conditions. In addition, the first FDASs of N+ and N – present a negative peak at 725 and 735 nm, respectively, indicating that the main acceptors are the higher-energy red Chls under nitrogen-enriched conditions and the lower-energy red Chls under nitrogen depletion. In contrast, the negative peak in the second FDAS (the 65–85 ps components in Fig. 4) almost coincides in both samples, and is assigned to the R3 band. In the third FDAS (the 220–280 ps components in Fig. 4), N+ exhibits a positive peak in the R2 band and a paired negative peak in the R3 band, whereas N – shows only the positive R2 peak. This indicates suppressed R2→R3 energy transfer under nitrogen-depleted conditions, which is further confirmed by the blue shift of the PSI fluorescence band in the seventh FDAS (the 16–20 ns components of Fig. 4). Specifically, high fluorescence in the R2 band implies that much of the excitation energy is emitted in that band rather than transferred from the R2 to the R3 band. It appears that the R1→R3 energy transfer compensates the suppressed R2→R3 energy transfer. In the fourth and fifth FDAS (the 1.1–1.7 ns and 4.8–5.1 ns components of Fig. 4, respectively), both samples exhibit a PSI peak at the same wavelength, which is assigned to the R3 band. These behaviors suggest that nitrogen depletion affects the initial excitation–relaxation process, but does not influence the relaxation processes once the energy has transferred to the R3 band.

In the PSII region of the delayed fluorescence spectra, the spectral shape is quite similar for both samples. Within PSII, energy transfers from CP43 to CP47 when the PSII reaction center combines with the core antenna complexes (Yokono et al. 2012b). If the nutrient condition alters the energy-transfer process between CP43 and CP47, it will change the spectral shape of the delayed fluorescence spectra in the PSII region. The similar delayed spectra in the present result indicate that nitrogen depletion does not affect the excitation energy transfer within PSII.

Excitation energy-transfer process between the pigment–protein complexes

The decreased relative amount of PBS may affect the excitation energy balance between PSI and PSII and the transfer process of the excitation energy between the pigment–protein complexes. We first consider the excitation energy-transfer processes involved in PSII (which donates energy to PSI and accepts it from PBS). In the first FDAS (the 10–20 ps components of Fig. 4), the amplitudes around 685 nm are positive in N+ but negative in N–. When the amplitudes in the first FDAS (~685 nm) are positive, the PSII→PSI energy transfer dominates the PBS→PSII energy transfer; negative amplitudes imply the opposite case. Therefore, nitrogen depletion suppresses the PSII→PSI energy transfer and enhances the PBS→PSII energy transfer.

The PSII→PSI energy transfer can be recognized from the PSI/PSII ratio in the delayed fluorescence, which originates from an excited state that is regenerated by charge recombination (Mimuro et al. 2007; Yokono et al. 2011). Both samples exhibit delayed fluorescence in the PSII and PSI fluorescence regions (Fig. 4), suggesting that PSII→PSI energy transfer occurs under nitrogen-deficient conditions. Table 2 shows the PSI/PSII fluorescence intensity ratios in the delayed and steady-state fluorescence spectra of *A. variabilis* cells grown under different nitrogen conditions. Here, we considered the differences in fluorescence quantum yield and divided the apparent PSI/PSII ratios by the corresponding mean lifetimes, as reported previously (Yokono et al. 2011). Although PSII→PSI energy transfer occurred in both samples, the PSI/PSII ratio in the delayed fluorescence spectra was 3.8 in N+ and 1.8 in N–. A larger PSI/PSII ratio in the delayed fluorescence spectra indicates a more energetic connection between PSII and PSI (in the PSII–PSI supercomplex), and greater PSII→PSI energy transfer (Yokono et al. 2011).

Under nitrogen deprivation, suppressed PSII→PSI energy transfer is supported not only by the decreased PSI/PSII ratio in the delayed fluorescence spectra of N−, but also by the decreased PSI/PSII fluorescence intensity ratio in the steady-state fluorescence spectra excited at 440 nm (Fig. 2a).

After PBS excitation at 600 nm, both nitrogen-enriched and nitrogen-depleted samples emitted fluorescence from their PSII and PSI red Chls (Fig. 2b). This fact indicates that both PSII and PSI terminally trap the excitation energy absorbed by PBS. In the steady-state fluorescence spectra excited at 600 nm, the PSI/PSII increases when PSI can receive more energy from PBS. PBS excitation at 600 nm can be followed by two possible pathways: direct PBS→PSI energy transfer (Fig. 5a) (Mullineaux 1992) or PBS→PSII energy transfer followed by PSII→PSI energy transfer (PBS→PSII→PSI energy transfer) (Fig. 5b) (Ley and Butler 1976; Bruce et al. 1985). The latter pathway is also detectable in the delayed fluorescence spectra, because the PSII–PSI supercomplex containing PBS (the PBS–PSII–PSI supercomplex) contributes to both the steady-state fluorescence excited at 600 nm and the delayed fluorescence. In the present study, the PSI/PSII ratios of N+ and N − were 4.8 and 2.7, respectively, in the steady-state fluorescence spectra excited at 600 nm, and 3.8 and 1.8, respectively, in the delayed fluorescence spectra (Table 2). To remove the effect of the PBS–PSII–PSI supercomplex (Akimoto et al. 2013), we computed the PSI/PSII ratio differences between the steady-state and delayed fluorescence (ΔPSI/PSII) (Table 2). The ΔPSI/PSIIs were similar in N+ and N–, suggesting that after adaptation to nitrogen-free medium, the PSI/PSII ratios in the delayed and steady-state fluorescence spectra were decreased by the reduced contribution of the PBS–PSII–PSI supercomplex in the *A. variabilis* filaments. Meanwhile, the contribution of the PBS–PSI supercomplex was not seriously affected.

Summary

Using steady-state and time-resolved spectroscopies, we investigated the energy-transfer dynamics in intact *A. variabilis* filaments grown under nitrogen-replete and nitrogen-depleted conditions for 6 months. The filaments grown in nitrogen-free medium altered their pigment compositions and excitation energy-transfer processes within and between the pigment–protein complexes. Although the PBS degraded under the nitrogen-depleted condition, the fast PC→APC energy-transfer path was maintained in PBS. Similarly, the excitation energy transfer in PSII was unaffected by nitrogen depletion. Conversely, there were three notable changes in PSI: (1) appearance of a specific red-Chl band (R1 band), (2) alterations (from R2 to R1) of the red Chls, which are the main energy mediators between antenna and R3, and (3) suppressed energy transfer between red Chls (R2–R3 energy transfer). Nitrogen depletion notably suppressed the PBS→PSII→PSI energy transfer between the pigment–protein complexes, and less severely affected the PBS→PSI energy transfer.

We previously discussed changes in energy-transfer processes during 15 days after the nitrogen depletion (Onishi et al. 2015). In the present study, we carried out measurements 4 days after final inoculation. Therefore, comparison between the 4-days filaments in the previous study (Onishi et al. 2015) and N– in the present study gives us information on differences between responses to nitrogen starvation during a short period (4 days after depletion) and those during a long period (6 months after depletion). The absolute values of the PSI/PSII ratios in the steady-state and delayed fluorescence spectra of the 4 days filaments were 2.0 and 3.2, respectively, resulting in ΔPSI/PSII = −1.2. This value is considerably smaller than that of N–, 0.9 (Table 2). Therefore, it can be concluded that, in a short period after nitrogen depletion, the PSII–PSI supercomplex (Fig. 5c) plays an important role in energy-transfer processes toward PSI (Fig. 5). This is probably due

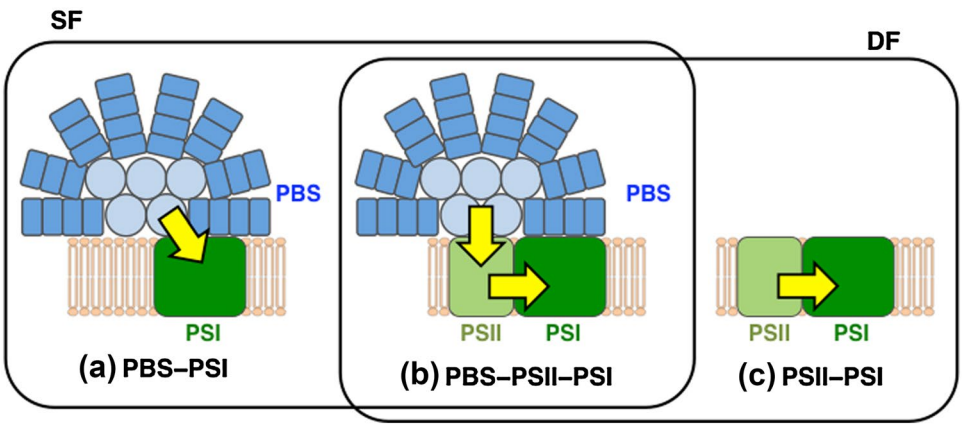

Fig. 5 Energy-transfer processes toward PSI, detected by the steady-state fluorescence excited at 600 nm (SF) and the delayed fluorescence (DF): PBS→PSI energy transfer (**a**), PBS→PSII→PSI energy transfer (**b**), PSII→PSI energy transfer (**c**)

to degradation of the PBS–PSI supercomplex (Fig. 5a) and PBS–PSII–PSI supercomplex (Fig. 5b) into the PSI complex and the PSII–PSI supercomplex (Fig. 5c), respectively, to use PBS as a source of nitrogen in an initial period after nitrogen depletion. The energy-transfer processes might not be optimized within 4 days after nitrogen depletion. There are few differences in energy transfer within PSI.

Acknowledgements This work was supported in part by JSPS KAKENHI Grant Number 16H06553 to S. Akimoto.

References

Akimoto S, Yokono M, Hamada F, Teshigahara A, Aikawa S, Kondo A (2012) Adaptation of light-harvesting systems of *Arthrospira platensis* to light conditions, probed by time-resolved fluorescence spectroscopy. Biochim Biophys Acta 1817:1483–1489

Akimoto S, Yokono, A, Aikawa S, Kondo A (2013) Modification of energy transfer processes in the cyanobacterium *Arthrospira platensis* to adapt to light conditions, probed by time-resolved fluorescence spectroscopy. Photosynth Res 117:235–243

Allen JF, Holmes NG (1986) A general model for regulation of photosynthetic unit function by protein phosphorylation. FEBS Lett 202:175–181

Allen MM, Smith AJ (1969) Nitrogen chlorosis in blue-green algae. Arch Microbiol 69:114–120

Arba M, Aikawa S, Niki K, Yokono M, Kondo A, Akimoto S (2013) Differences in excitation energy transfer of Arthrospira platensis cells grown in seawater medium and freshwater medium, probed by time-resolved fluorescence spectroscopy. Chem Phys Lett 588:231–236

Berman-Frank I, Lundgren P, Falkowski P (2003) Nitrogen fixation and photosynthetic oxygen evolution in cyanobacteria. Res Microbiol 154:157–164

Blankenship RE (2014) Molecular mechanisms of photosynthesis, 2nd edn. Wiley-Blackwell.

Boardman NK, Thome SW, Anderson JM (1966) Fluorescence properties of particles obtained by digitonin fragmentation of spinach chloroplasts. Proc Natl Acad Sci USA 56:586–593

Bruce D, Biggins J, Steiner T, Thewalt M (1985) Mechanism of the light state transition in photosynthesis. IV. Picosecond fluorescence spectroscopy of *Anacystis nidulans* and *Porphyridium cruentum* in state 1 and state 2 at 77 K. Biochim Biophys Acta 806:237–246

Cobb HD, Myers J (1964) Comparative Studies of Nitrogen Fixation and Photosynthesis in *Anabaena cylindrical*. Am J Bot 51(7):753–762

Collier JL, Grossman AR (1992) Chlorosis induced by nutrient deprivation in *Synechococcus* sp. strain PCC 7942: Not all bleaching is the same. J Bacteriol 174:4718–4726

Collier JL, Herbert SK, Fork DC, Grossman AR (1994) Changes in the cyanobacterial photosynthetic apparatus during acclimation to macronutrient deprivation. Photosynth Res 42:173–183

Ehira S, Ohmori M (2006) NrrA, a nitrogen-responsive response regulator facilitates heterocyst development in the cyanobacterium *Anabaena* sp. strain PCC 7120. Mol Microbiol 59:1692–1703

Fay P (1992) Oxygen relations of nitrogen fixation in cyanobacteria. Microbiol Rev 56:340–373

Ferimazova N, Felcmanova K, Setlikova E, Küpper H, Maldener I, Hauska G, Sediva B, Prasil O (2013) Regulation of photosynthesis during heterocyst differentiation in *Anabaena* sp strain PCC 7120 investigated in vivo at single-cell level by chlorophyll fluorescence kinetic microscopy. Photosynth Res 116:79–91

Fogg GE (2001) Algal Adaptation to Stress. In: Rai LC, Gaur JP (eds) Algal Adaptation to Environmental Stresses: Physiological, Biochemical and Molecular Mechanism. Springer-Verlag, Berlin/Heidelberg, pp 135–171

Gantt E (1975) Phycobilisomes: Light-harvesting pigment complexes. Bioscience 25:781–788

Gantt E, Conti SF (1969) Ultrastructure of blue-green algae. J Bacteriol 97:1486–1493

Goedheer JC (1972) Fluorescence in relation to photosynthesis. Ann Rev Plant Physiol 23:87–112

Görl M, Sauer J, Baier T, Forchhammer K (1998) Nitrogen-starvation-induced chlorosis in *Synechococcus* PCC 7942: adaptation to long-term survival. Microbiology 144:2449–2458

Govindjee, Yang L (1966) Structure of the red fluorescence band in chloroplasts. J Gen Physiol 49:763–780

Govindjee (2004) Chlorophyll a fluorescence: A bit of basics and history. In: Papageorgiou GC, Govindjee (eds) Chlorophyll a fluorescence: a signature of photosynthesis. Kluwer Academic Publishers, Dordrecht, pp 1–42

Grossman AR, Schaefer MR, Chiang GG, Collier JL (1993) The phycobilisome, a light-harvesting complex responsive to environmental conditions. Microbiol Rev 57:725–749

Grossman AR, Schaefer MR, Chiang GG, Collier JL (1994) The responses of cyanobacteria to environmental conditions. In: Bryant DA (ed) The molecular biology of cyanobacteria. Kluwer Academic Publishers, Dordrecht, pp 641–675

Jordan P, Fromme P, Witt HT, Klukas O, Saenger W, Krauß N (2001) Three-dimensional structure of cyanobacterial photosystem I at 2.5 Å resolution. Nature 411:909–917

Kumar K, Mella-Herrera RA, Golden JW (2010) Cyanobacterial heterocysts. Cold Spring Harb Perspect Biol 2:a000315

Laudenbach DE, Straus NA (1988) Characterization of a cyanobacterial iron stress-induced gene similar to *psbC*. J Bacteriol 170:5018–5026

Ley AC, Butler WL (1976) Efficiency of energy transfer from photosystem 11 to photosystem 1 in *Porphyridium cruentum*. Proc Natl Acad Sci USA 73:3957–3960

Maldener I, Muro-Pastor AM (2010) Cyanobacterial heterocysts. In: Encyclopedia of life sciences (ELS). Wiley, New York

Michel KP, Pistorius EK (2004) Adaptation of the photosynthetic electron transport chain in cyanobacteria to iron deficiency: The function of IdiA and IsiA. Physiol Plant 120:36–50

Mimuro M, Katoh T (1991) Carotenoids in photosynthesis: absorption, transfer and dissipation of light energy. Pure Appl Chem 63:23–130

Mimuro M, Akimoto S, Tomo T, Yokono M, Miyashita H, Tsuchiya T (2007) Delayed fluorescence observed in the nanosecond time region at 77 K originates directly from the photosystem II reaction center. Biochim Biophys Acta 1767: 327–334

Mullineaux CW (1992) Excitation energy transfer from phycobilisomes to photosystem I in a cyanobacterium. Biochim Biophys Acta 1100:285–292

Murata N, Satoh K (1986) Absorption and fluorescence emission by intact cells, chloroplasts, and chlorophyll–protein complexes. In: Govindjee Amesz J, Fork DC (eds) Light emission by plants and bacteria, pp 137–159. Academic Press

Nakayama K, Yamaoka T, Katoh S (1979) Chromatographic separation of photosystems I and II from the thylakoid membrane isolated from a thermophilic blue-green alga. Plant Cell Physiol 20:1565–1576

Niki K, Aikawa S, Yokono M, Kondo A, Akimoto S (2015) Differences in energy transfer of a cyanobacterium, *Synechococcus* sp. PCC 7002, grown in different cultivation media. Photosynth Res 125:201–210

Onishi A, Aikawa S, Kondo A, Akimoto S (2015) Energy transfer in *Anabaena variabilis* filaments under nitrogen depletion, studied by time-resolved fluorescence. Photosynth Res 125:191–199

Pålsson LO, Flemming C, Gobets B, Grondelle R, Dekker JP, Schlodder E (1998) Energy transfer and charge separation in photosystem I: P700 oxidation upon selective excitation of the long-wavelength antenna chlorophylls of *Synechococcus elongates*. Biophys J 74:2611–2622

Peter P, Sarma AP, Hasan MDA, Murthy SDS (2010) Studies on the Impact of nitrogen starvation on the photosynthetic pigments through spectral properties of the cyanobacterium, *Spirulina platensis*: Identification of target phycobiliprotein under nitrogen chlorosis. Bot Res Intl 3: 30–34

Postgate J (1998) The origins of the unit of nitrogen fixation at the University of Sussex. Notes Rec R Soc Lond 52:355–362

Schwarz R, Forchhammer K (2005) Acclimation of unicellular cyanobacteria to macronutrient deficiency: emergence of a complex network of cellular responses. Microbiology 151:2503–2514

Takaichi S, Mochimaru M, Maoka T (2006) Presence of free myxol and 4-hydroxymyxol and absence of myxol glycosides in *Anabaena variabilis* ATCC 29413, and proposal of a biosynthetic pathway of carotenoids. Plant Cell Physiol 47:211–216

Thomas J (1970) Absence of the pigments of photosystem II of photosynthesis in heterocysts of blue–green alga. Nature 228:181–183

Trissl HW (1993) Long-wavelength absorbing antenna pigments and heterogeneous absorption bands concentrate excitons and increase absorption cross section. Photosynth Res 35:247–263

Wolk CP (1996) Heterocyst formation. Annu Rev Genet 30:59–78

Ying L, Huang X, Huang B, Xie J, Zhao J, Zhao XS (2002) Fluorescence emission and absorption spectra of single *Anabaena* sp. strain PCC7120 cells. Photochem Photobiol 76:310–313

Yokono M, Murakami A, Akimoto S (2011) Excitation energy transfer between photosystem II and photosystem I in red algae: Larger amounts of phycobilisome enhance spillover. Biochim Biophys Acta 1807:847–853

Yokono M, Uchida H, Suzawa Y, Akiomoto S, Murakami A (2012a) Stabilization and modulation of the phycobilisome by calcium in the calciphilic freshwater red alga Bangia atropurpurea. Biochim Biophys Acta 1817:306–311

Yokono M, Tomo T, Nagao R, Ito H, Tanaka A, Akimoto S (2012b) Alterations in photosynthetic pigments and amino acid composition of D1 protein change energy distribution in photosystem II. Biochim Biophys Acta 1817:754–759